

Cell Lines

Human cervical carcinoma HeLa cells were supplied from Japanese Collection of Research Bioresources Cell Bank (Osaka, Japan). HeLa cells were maintained in Dulbecco's Modified Eagle Medium (DMEM; Sigma Chemical Co., Inc.) containing 10% fetal bovine serum in a humidified atmosphere containing 5% CO₂ at 37°C.

Synthesis of Thiolated Camptothecin (CPT-DP)

A CPT derivative bearing the pyridyl disulfide group was synthesized as shown in Fig. 2. Briefly, a solution of methoxycarbonylsulfonyl chloride (1.25 g, 3.8 mmol) in methylene chloride (26 ml) was treated with 3-mercaptopropionic acid (1.05 g, 3.8 mmol) in methylene chloride (13 ml) for 2 h. After solvent was evaporated, the residue was redissolved in methylene chloride (26 ml) and treated dropwise with a solution of 2-mercaptopyridine (1.1 g, 3.8 ml) in 13 ml of the same solvent. After stirring overnight, the solvent was evaporated to yield an oily residue of 3-(2-pyrinyldithio)propionic acid. Then, 0.5 mmol of 3-(2-pyrinyldithio)propionic acid was mixed with 0.5 mmol CPT, 0.55 mmol DMAP and 0.55 mmol EDC in 5 ml methylene chloride. After 24 h stirring at room temperature, the mixture was diluted with 150 ml methylene chloride and washed with 0.01 N HCl (30 ml, one time) and water (30 ml, six times). The organic layer was evaporated to obtain a pale orange solid. The product was purified by silica gel chromatography using methylene chloride-methanol (97:3 v/v) as an eluent to yield an orange solid of CPT-DP. The proper modification of CPT was analyzed by ¹H-NMR in DMSO at 25°C

Synthesis of Thiolated Poly(ethylene glycol)-Poly(glutamic acid) [PEG-b-P(Glu-DP)] Block Copolymer

Preparation of Disulfide Amine Linker

Thiopyridyl disulfide was dissolved in 20 ml of methanol and 0.8 ml of acetic acid. Into this solution was added

dropwise over a period of 0.5 h 2-aminoethylthiol hydrochloride in 10 ml methanol. The mixture was stirred for 48 h and then evaporated to yield yellow oil, followed by washing with 50 ml diethyl ether and dissolution in 10 ml of methanol. The product was precipitated by addition of 200 ml of diethyl ether, chilled for 12 h at -20°C and collected by vacuum filtration (yield: 77%).

Synthesis of Poly(ethylene glycol)-Poly(glutamic acid) [PEG-b-P(Glu)] Block Copolymer

PEG-P(Glu) block copolymer was synthesized according to the previously described synthetic method (27). Briefly, the *N*-carboxy anhydride of γ -benzyl L-glutamate (BLG-NCA) was synthesized by the Fuchs-Farthing method using triphosgene. Then, BLG-NCA was polymerized in DMF, initiated by the primary amino group of CH₃O-PEG-NH₂, to obtain PEG-poly(γ -benzyl L-glutamate) (PEG-b-PBLG) block copolymer. The molecular weight distribution of PEG-b-PBLG was determined by gel permeation chromatography [column: TSK-gel G3000HHR, G4000HHR (Tosoh Co., Inc., Yamaguchi, Japan); eluent: DMF containing 10 mM LiCl; flow rate—0.8 ml/min; detector: refractive index; temperature: 25°C]. The polymerization degree of PBLG was verified by comparing the proton ratios of the methylene units in PEG (-OCH₂CH₂-; δ = 3.7 ppm) and the phenyl groups of PBLG (-CH₂C₆H₅; δ = 7.3 ppm) in ¹H-NMR spectrum (solvent: DMSO-d₆; temperature: 80°C), and it was determined to be 81. The deprotection of the benzyl group of PEG-b-PBLG was carried out by mixing with 0.5 N NaOH at room temperature to obtain PEG-P(Glu).

Synthesis of Thiolated Poly(ethylene glycol)-b-Poly(glutamic acid) [PEG-b-P(Glu-DP)] Block Copolymer

The P(Glu) backbone of PEG-b-P(Glu) was thiolated by the procedure illustrated in the Fig. 3. Briefly, PEG-b-P(Glu) was dissolved in DMSO, followed by addition of NHS and water soluble DCC. The solution was stirred for 2 h, and

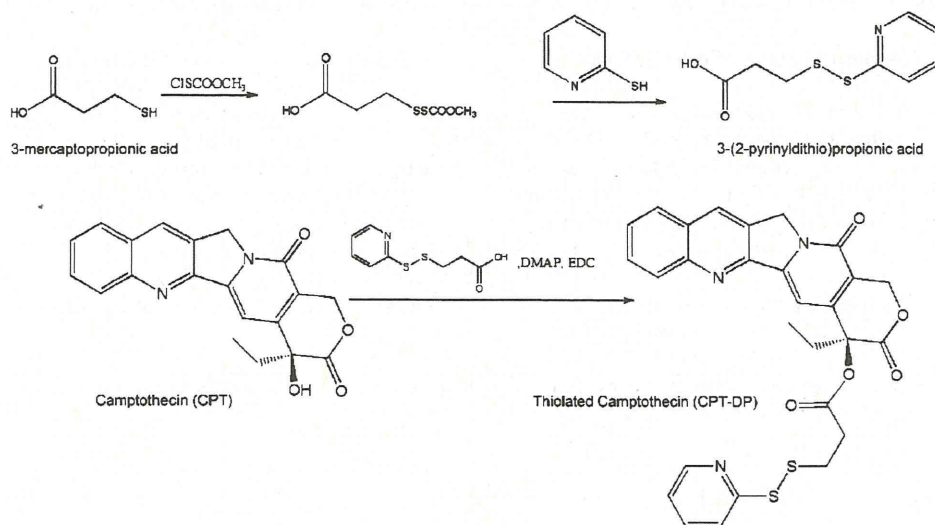


Fig. 2. Synthesis of CPT-DP.

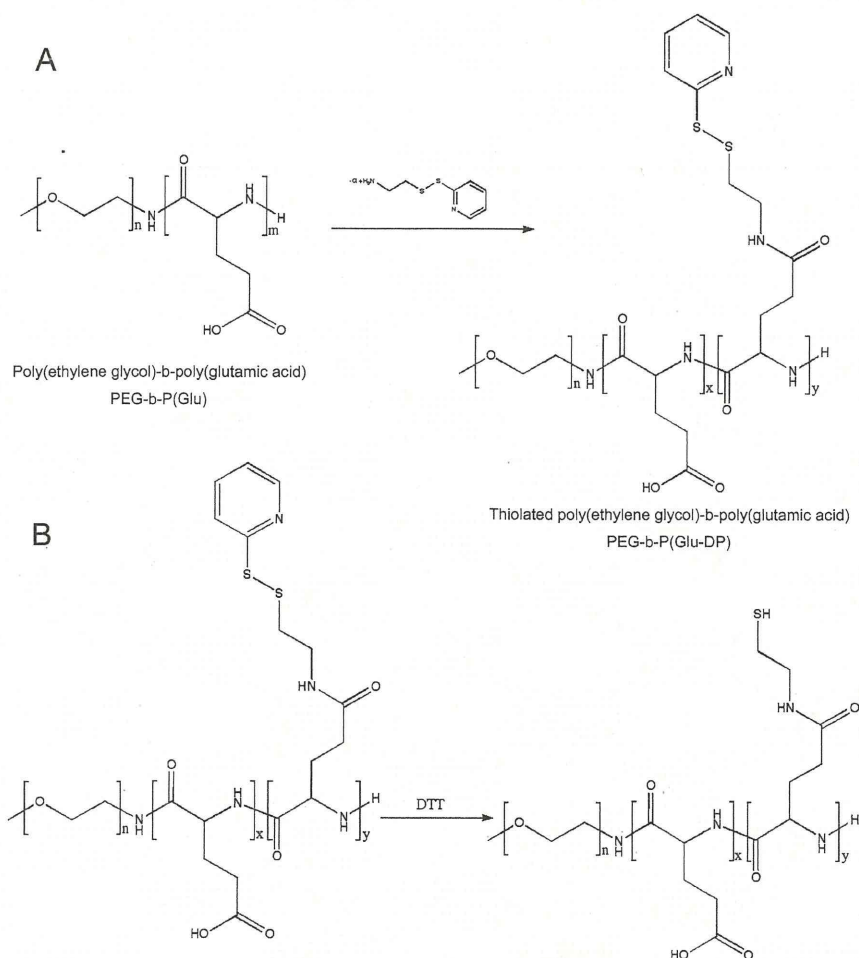


Fig. 3. A Synthesis of thiolated (PEG-*b*-P(Glu-DP)) B Deprotection of PEG-*b*-P(Glu-DP) using DTT.

then SPTDP was added. The solution was stirred for another 20 h. Then, the mixture was dialyzed against water and finally freeze-dried. The characterization of the polymer was performed by $^1\text{H-NMR}$ (solvent: DMSO- d_6 ; temperature: 80°C).

Preparation of Camptothecin-loaded Micelle (CPT/m)

CPT/m were prepared as follows: PEG-*b*-P(Glu-DP) (60 mg) was mixed with DTT (3-fold excess) in DMSO in order to deprotect the sulfide group at the *p*(Glu) backbone. Twenty-four hours later, the solution was dialyzed against DMSO. After dialysis, CPT-DP, (40 mg) was added and the solution was shaken at 37°C in dark for 72 h. Then, the unreacted CPT-DP was removed by dialysis against DMSO. The resulting drug-polymer conjugate was dialyzed against water in order to form polymeric micelles. Finally, the micelle solution was purified by ultrafiltration (MWCO—50,000) and the size distribution of the micelle was measured by dynamic light scattering (DLS) using a Zetasizer Nano ZS90 (Malvern Instruments Ltd., Worcestershire, United Kingdom). The CPT concentration of micelle solution was determined by reverse phase liquid chromatography (RPLC) [column: μ -Bondasphere (Waters, Japan); eluent: acetonitrile/1% acetic acid; detector: fluorescence (emission—370 nm; detection—

440 nm); temperature: 40°C] after micelle dissociation with 10 mM DTT and mixing in 1 N HCl.

Synthesis of Dendrimer Phthalocyanine

The synthesis of the ionic DPc was performed according to the method reported by Ng's group (28). The second generation of dendritic phenol was reacted with 4-nitrophthalonitrile by an alkali-mediated coupling reaction to obtain the corresponding dendritic phthalonitrile, which was treated with $\text{Zn}(\text{OAc})_2$ and 1,8-diazabicyclo[5.4.0]undec-7-ene (DBU) in *n*-pentanol to give DPc. The obtained DPc was 4,904 dalton and the adsorption spectra in an aqueous solution revealed that DPc exhibits a B band absorption at 350 nm and a strong Q band absorption at 685 nm, indicating a monomeric dispersion (24).

Synthesis of Poly(ethylene glycol)-*b*-poly(L-Lysine) [PEG-*b*-PLL]

PEG-*b*-PLL block copolymer was synthesized as previously reported (29). Briefly, the *N*-carboxy anhydride of *N*-Z-Lysine was polymerized from the ω - NH_2 group of $\text{CH}_3\text{O-PEG-NH}_2$ in DMF under Ar to obtain PEG-*b*-PLL(Z), followed by the

deprotection of the Z group. The polymerization degree of the PLL segments was determined to be 49 by $^1\text{H-NMR}$.

Preparation of Dendrimer Phthalocyanine-loaded Micelle

The DPc/m was prepared as previously described (24). Briefly, DPc was dissolved in 10 mM Na_2HPO_4 (1 ml) and added to PEG-*b*-PLL in a 10 mM NaH_2PO_4 (0.457 ml) to give a solution containing DPc/m in 10 mM phosphate buffered solution (pH 7.4). The size distribution of DPc/m was determined by DLS.

CTP Release from CPT/m under Different Conditions

The release of CPT from the micelle under different conditions was evaluated by the dialysis method. Briefly, a micellar solution of known CPT concentration was placed inside a dialysis bag and dialyzed against 10 mM PBS plus 150 mM NaCl (pH 5 and 7.4) or 10 mM PBS plus 3 mM DTT at 37°C. The solution outside the dialysis bag was sampled at defined time periods to determine the amount of free CPT released from the micelle. Then, 0.1 ml of the sample was diluted in 0.4 ml of 1 N HCl, and the concentration was measured by RPLC using the conditions previously described.

In Vitro Photocytotoxicity of DPc/m

In order to determine the non-toxic concentration of DPc/m that will be used for the PCI of CPT/m, the growth-inhibitory activity of the DPc/m was evaluated by MTT assay. HeLa cells were cultured in DMEM containing 10% FBS in 96-well multiplate. After 24 h incubation, cells were incubated with the drugs for 24 h, followed by photoirradiation for 10 min using a 300 W halogen lamp (fluence rate: 3.0 mW cm^{-2}) equipped with a band-pass filter (400–700 nm). Then, the cells were post-incubated for 24 and 48 h. The cell viability was measured by MTT assay.

PCI-enhanced In Vitro Cytotoxicity of Camptothecin-loaded Micelle

The growth-inhibitory activity of the free CPT, free CPT-DP and CPT/m with and without a non-toxic concentration of DPc/m was evaluated by MTT assay. HeLa cells were cultured in DMEM containing 10% FBS in 96-well multiplate. After 24 h incubation, the cells were exposed to each CPT formulation in the combination with DPc/m. Twenty-four hours after drug exposure, the cells were photoirradiated 10 min. Then, the cells were post-incubated for 24 and 48 h. Finally, MTT solution was added and, 3 h later, 20% SDS solution was added. Cell viability was measured by the formed formazan absorbance at 570 nm.

RESULTS

CPT-loaded Micelle

The proper incorporation of the linkers to CPT and PEG-*b*-P(Glu) was confirmed by $^1\text{H-NMR}$. After column purification, the spectra of CPT-DP presented the proton peaks corresponding to the CPT plus the alkyl-disulfide-pyridine

linker (Fig. 4). From the proton ratio between the methylene group *j* of CPT (Fig. 4A) and the methylene protons, 1 or 2, of the conjugated linker, the degree of modification of CPT was determined to be 100% by $^1\text{H-NMR}$ (Fig. 4B). Moreover, the RPLC results showed a single peak suggesting high purity of the product (Fig. 4C). For the PEG-*b*-P(Glu-DP), the degree

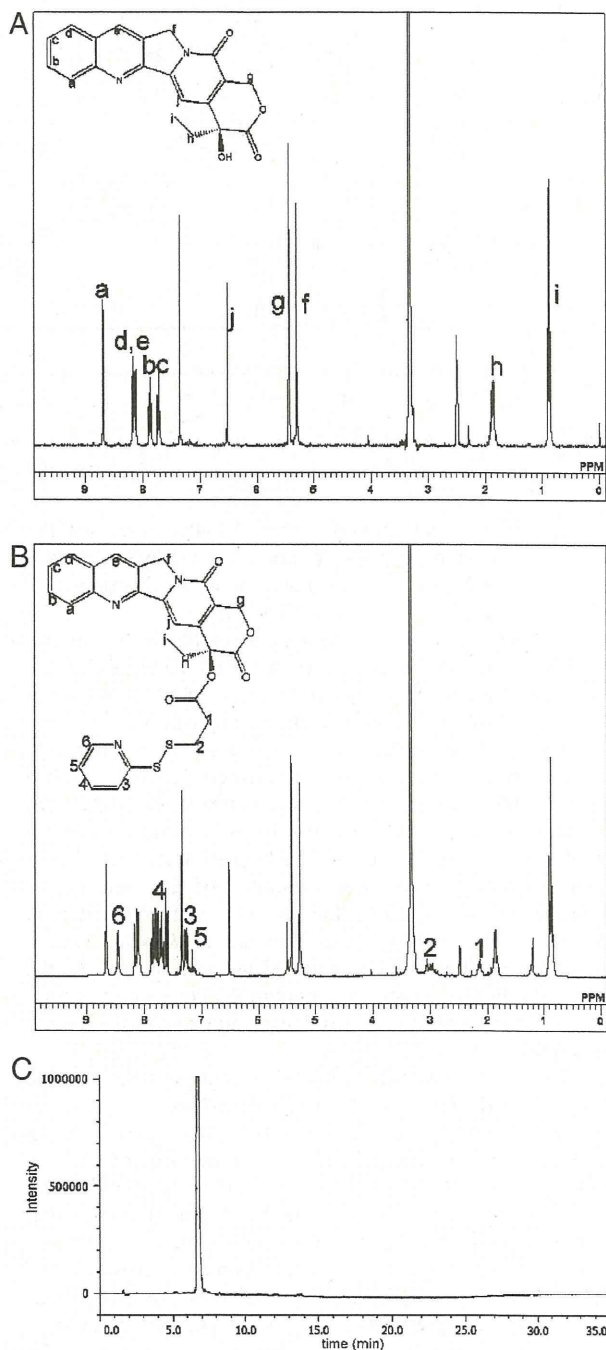


Fig. 4. Characterization of the thiolated camptothecin derivative. **A** $^1\text{H-NMR}$ spectra of CPT; **B** $^1\text{H-NMR}$ spectra of thiolated camptothecin (CPT-DP); **C** RPLC chromatogram of CPT-DP.

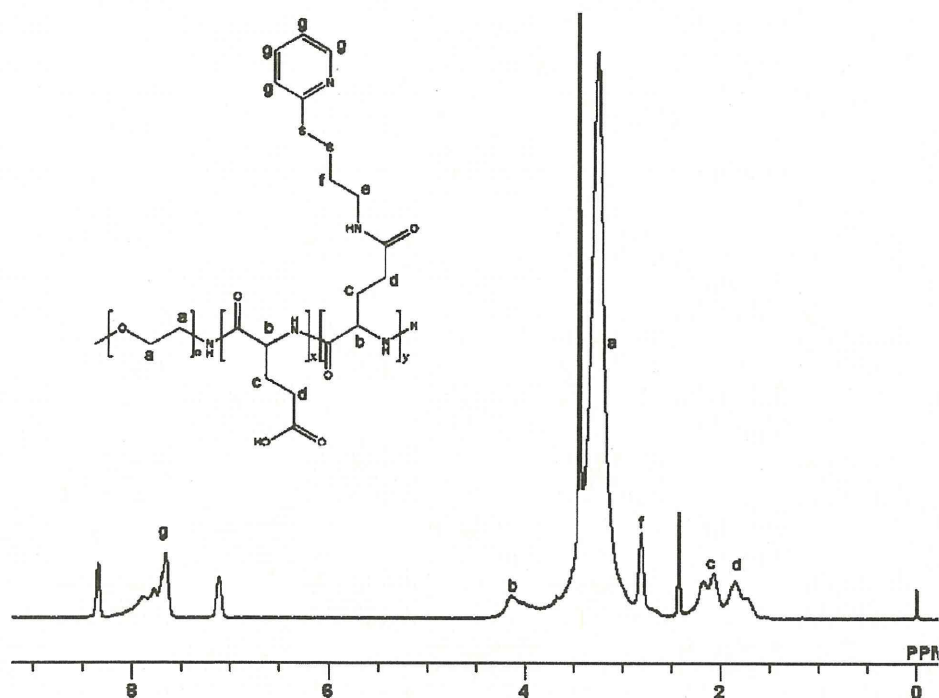


Fig. 5. $^1\text{H-NMR}$ spectra of thiolated poly(ethylene glycol)-poly(glutamic acid) block copolymer (PEG-*b*-P(Glu-DP)).

of thiolation was determined to be 44 [54% of the P(Glu) units] by comparing the proton ratios of the methylene units in PEG ($-\text{OCH}_2\text{CH}_2-$; $\delta=3.7$ ppm) and the pyridine groups of P(Glu-DP) ($-\text{CH}_2\text{H}_4\text{N}$; $\delta=7.5$ ppm; Fig. 5).

The driving force for micelle assembly is the hydrophobic interaction between P(Glu-DP) backbones of the block copolymers after the conjugation of CPT-DP. After purification of the micelles by ultrafiltration, the size distribution of CPT/m was determined to be 96.3 nm with a considerable low cumulant polydispersity ($\mu_2/\Gamma^2=0.048$) by DLS. In addition, the CPT/m formulation offers the possibility to be lyophilized for long-term storage. After redissolving the freeze-dried CPT/m in water, the DLS results showed a *z*-average diameter of 100 nm and a polydispersity of 0.1. Note that the size of a colloidal drug carrier is a determinant feature of its fate in blood circulation and its biodistribution. The sub-100 nm size as well as the hydrophilic PEG palisade surrounding the core are important features of the CPT/m to avoid their uptake by the reticuloendothelial system.

The drug loading was estimated after micelle dissociation with 10 mM DTT by RPLC. The incorporated amount was determined to be 0.25 CPT molecules per thiol group at the p(Glu) backbone ($[\text{CPT-S}]/[\text{SH}]$), indicating 20% of CPT to PEG-*b*-P(Glu-DP) (*w/w*). This corresponds to approximately 35% of the initial CPT-DP feeding. Worth mentioning is that the thiol moieties in the P(Glu-DP) backbone that did not react with CPT may form disulfide bonds to crosslink the micellar core. We previously reported that similar micellar systems show complete disulfide bond formation by spontaneous oxidation of the thiol groups in the solution (30–32). Such disulfide crosslinks may stabilize the micelle structure in addition to the hydrophobic interaction.

Release Rate from CPT/m under Different Conditions

Drug-loaded micelles should be designed to release their contents after reaching the targeted tissue since the premature drug release can lead to toxic effects. Hence, the CPT release rate was studied under different conditions simulating different biological environments (Fig. 6). At settings that reproduce the extracellular environments, i.e. 10 mM phosphate buffer pH 7.4 plus 150 mM NaCl, the CPT release from the micelle was extremely low. After 96 h, the release was determined to be almost 30% of the incorporated CPT (Fig. 6). At endosomal pH, i.e. pH 5.5, the percentage of drug released from the micelle core was also found to be very low with approximately 1% of the drug released after 96 h (Fig. 6). Nevertheless, in a reductive environment simulating the cytosolic conditions, 10 mM PBS plus 3 mM DTT, a burst release of CPT was observed throughout the first 10 h. During this period, almost 80% of the incorporated drug was released. Then, the drug release reached a plateau achieving more than 90% of the drug released in 96 h (Fig. 6). This fast and preferential drug release under cytosolic conditions can be exploited to deliver CPT only in tissues where the micelles can escape from the endosomes aided by PCI.

In Vitro Photocytotoxicity of DPc/m

HeLa cells were incubated with different concentrations of DPc/m for 24 h. Then, HeLa cells were photoirradiated at the fluence rate of 3.0 mW/cm^2 for 10 min (fluence— 1.8 J/cm^2) and then post-incubated for 24 and 48 h. The results presented a DPc concentration-dependent decrease in cell viability (Fig. 7A and B). The photo-induced cell death is observed at the region of high DPc concentrations, and it

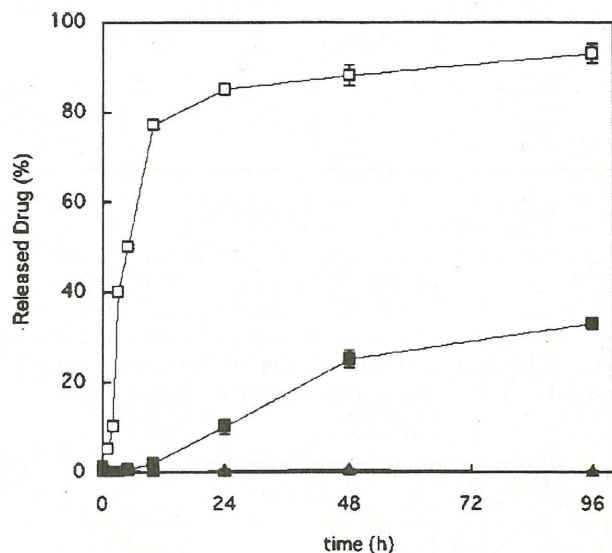


Fig. 6. Release rate of CPT-DP from the micelles (CPT/m) at 10 mM phosphate buffer plus 150 mM NaCl at pH 5.5 (filled triangle); pH 7.4 (filled square); and 3 mM DTT (unfilled square). Determined by RPLC (acetonitrile:1% acetic; fluorescence emission: 370 nm; fluorescence detection—440 nm). Data are shown as mean \pm SD ($n=3$).

might be attributable to the vast photochemical reactions. At low DPc concentrations, the production of reactive oxygen species may be low and mainly confined to the endosomal compartments, maintaining the cell viability. Thus, in order to minimize the photocytotoxicity from the DPc/m in the following PCI-mediated enhancement of CPT/m, a non-toxic concentration of DPc/m was determined. The highest non-toxic concentration of dendrimer-micelle was observed at 1×10^{-3} mg/ml. Therefore, the DPc/m concentration was fixed at 1×10^{-4} mg/ml for the following experiments.

PCI-Enhanced *In Vitro* Cytotoxicity of CPT/m

The cytotoxicity of free CPT, free CPT-DP and CPT/m in combination with the non-toxic concentration of DPc/m with and without photoirradiation against HeLa cells is shown in Figs. 8 and 9, and IC₅₀ values are summarized in Table I. As shown in Fig. 8 and Table I, free CPT-DP showed slightly higher cytotoxicity than free CPT, which may be due to facilitated cellular uptake of CPT-DP with a hydrophobic pyridyl disulfide group. In the presence of photoirradiation, the combination of free CPT or CPT-DP and DPc/m showed less than 2-fold enhancement of the cytotoxicity without photoirradiation. Because free CPT or CPT-DP enter cells by passive diffusion and show potent cytotoxicity without photoirradiation, there may be a synergistic effect between cytotoxic compounds (i.e., free CPT and CPT-DP) and photodynamic effect by DPc/m. This effect is assumed to be the combination effect of chemotherapy and PDT rather than PCI, since PCI is aimed to deliver cell membrane-impermeable drugs and macromolecular compounds from the endo-/lysosomes to the cytosol through the photochemical disruption of endo-/lysosomal membranes, thus achieving the light-selective drug action (9). On the other hand, the combination of CPT/m and DPc/m without photoirradiation was not toxic after 24 h post-incubation, probably due to the localization of

the micelles in the endosome and the restricted drug release of CPT/m (Fig. 9A). However, when the cells were photoirradiated, the PCI effect exposed the CPT/m to the reductive conditions of the cytosol by endosomal escape. Hence, the *in vitro* cytotoxicity of CPT/m was considerably increased (Fig. 9A), suggesting that the antitumor activity of CPT/m can be significantly enhanced by photoirradiation. At 48 h, the combination of CPT/m and DPc/m without photoirradiation slightly decreased the cell viability at high CPT/m concentrations (Fig. 9B). Nevertheless, the PCI using DPc/m significantly enhanced the antitumor activity of CPT/m at 48 h (Fig. 9B). Thus, as shown in Table I, the combination of CPT/m and DPc/m achieved remarkable (6.5-fold or much more) enhancement of the cytotoxicity by photoirradiation.

DISCUSSION

Berg and Høgset *et al.* were the first to combine PCI and chemotherapy to deliberately increase the internalization of the anticancer drug bleomycin (33). The PCI-mediated relocation of bleomycin into the cytosol considerably enhanced its *in vitro* and *in vivo* efficacy because bleomycin is practically non-permeant to the plasma membrane and enters the cells by endocytosis whereby it may be degraded in the lysosomes. Nevertheless, bleomycin is in contrast to traditional anticancer agents, such as CPT, that will easily pass the cell membrane and will generally be taken up by non-target cells generating severe side effects. Therefore, the PCI site-specific targeting of traditional anticancer drugs should be performed using drug carriers that enter the cells *via* endocytosis and release their contents only after PCI. In this way, the CPT/m presented a strong *in vitro* cytotoxicity after endosomal escape by PCI. The carrier activation is correlated with the fast CPT release from the micelle core under reductive conditions. Moreover, the modification of the outer hydrophilic shell of CPT/m with cancer-specific ligands can increase the specific uptake in tumor cells and the efficiency will be considerably enhanced.

The CPT/m were also designed to release their contents after reaching the targeted tissue. Like this, the drug leakage from CPT/m during blood circulation will be minimized since the experiments of drug release rate demonstrated that the disulfide linker used to conjugate CPT to the block copolymer backbone is selectively cleaved under reductive conditions. This will reduce the toxic effects that arise from non-specific accumulation of free drug. Moreover, the delivery of the active lactone form of CPT is also crucial for exerting the antitumor activity. In this way, it has been determined that modifying CPT at the 20 position as an ester stabilizes the active lactone ring under physiological conditions (34). Accordingly, the CPT instability under physiological conditions may also be reduced for the CPT-DP derivative. In addition, previous studies revealed that the lactone ring of CPT was protected upon incorporation of the drug into the lipid bilayer of liposomes (35,36), microspheres (37,38), nanobiohybrids (39), and polymeric micelles (40,41). Thus, the hydrophobic core of CPT/m probably functions as an auspicious CPT reservoir by inhibiting drug inactivation. In addition, after the PCI, the CPT/m will reach the interior of cancer cells, release the CPT in the lactone form avoiding extracellular inactivation and, in this way, maximize the efficiency of CPT.

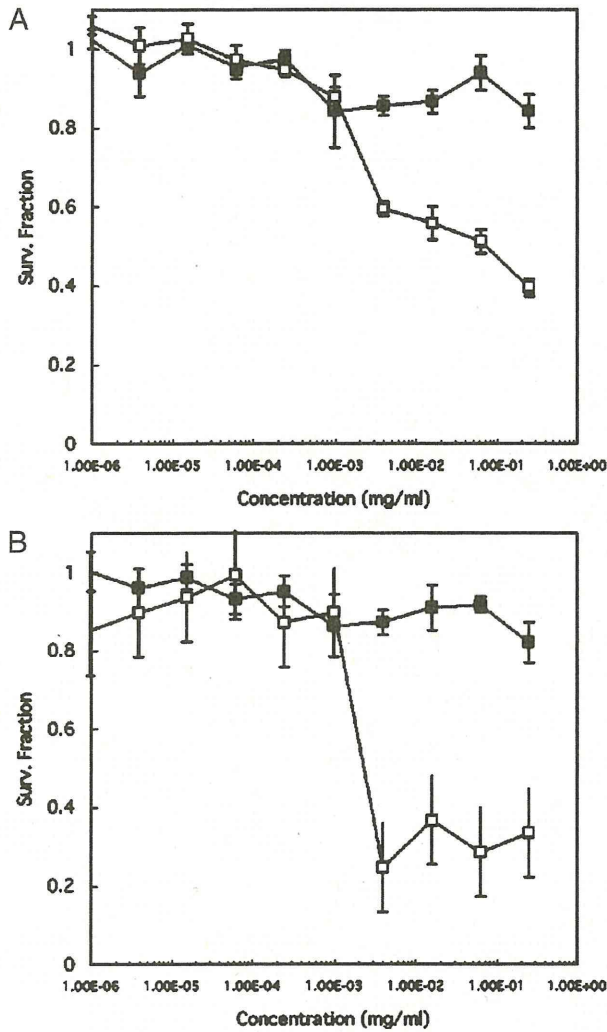


Fig. 7. Cell viability of dendrimer phthalocyanine-loaded polymeric micelles (DPc/m) without irradiation (filled square) and with 10 min irradiation at a fluence of 1.8 J/cm² (unfilled square). **A** 24 h incubation after photoirradiation; **B** 48 h incubation after photoirradiation. Data are shown as mean \pm SD ($n=4$).

In this study, we successfully achieved the light-induced activation of chemotherapeutic agents by the PCI using the combination of CPT/m and DPc/m under the condition at which the photosensitizer (PS) alone showed no photocytotoxicity. Although there are several previous reports regarding the photo-activated chemotherapy using the combination of chemotherapeutic agents and PSs, in those studies the light-induced enhancement of the cytotoxicity of chemotherapeutic agents was observed only when the PS alone showed significant photocytotoxicity (42,43). The highly light-selective activation of chemotherapeutic agents by our system may be attributed to (1) the aforementioned CPT release selectively after the endosomal escape of CPT/m by the PCI and (2) highly selective photodamage to the endo-/lysosomal compartments by DPc/m. It is reported that low-molecular weight PSs such as sulfonated phthalocyanine (AIPcS_{2a}), which were used in other studies, show significant photocytotoxicity accompanied by the PCI (8,9), probably because

they are assumed to accumulate not only in the endo-/lysosomes but also in other organelles susceptible to the photodamage such as the plasma membranes and mitochondria. In contrast, DPc/m is assumed to accumulate selectively in the endo-/lysosomes, thereby achieving the PCI without compromising the cytotoxicity. Regarding the intracellular behaviors of DPc/m upon photoirradiation, we previously reported that DPc/m showed 100-fold higher *in vitro* photocytotoxicity against HeLa cells than free DPc, which cannot be explained by four times higher cellular uptake of DPc/m compared with free DPc (24). Therefore, it appears that DPc/m in a micellar form should play a pivotal role in the intracellular photochemical reactions rather than released free DPc. Indeed, we confirmed that the physicochemical

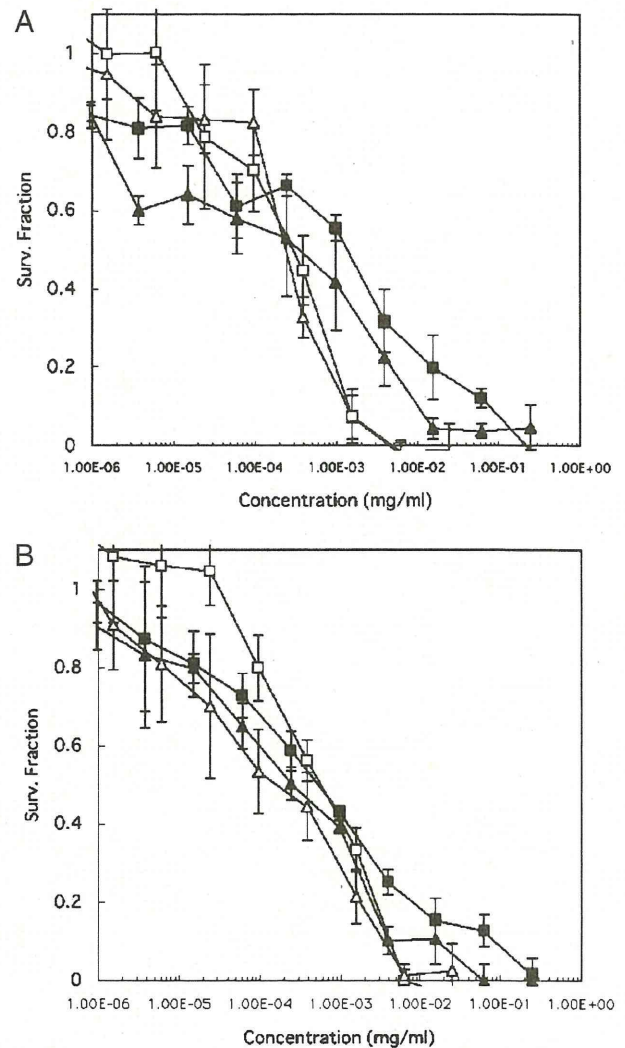


Fig. 8. Cell viability after treatment with CPT and CPT-DP combined with a non-toxic concentration of DPc/m with and without 10 min irradiation at a fluence of 1.8 J/cm². **A** 24 h incubation after photoirradiation; **B** 48 h incubation after photoirradiation. Non-photoirradiated CPT plus DPc/m, filled square; non-photoirradiated CPT-DP plus DPc/m, filled triangle; photoirradiated CPT plus DPc/m, unfilled square; photoirradiated CPT-DP plus DPc/m, unfilled triangle. Data are shown as mean \pm SD ($n=4$).

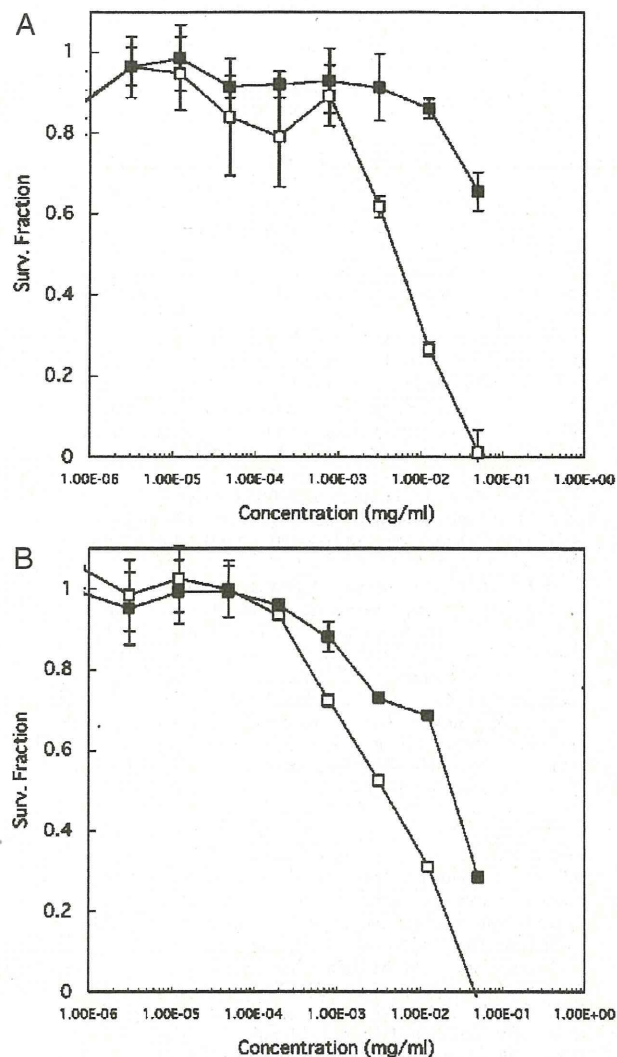


Fig. 9. Cell viability for CPT/m combined with a non-toxic concentration of DPc/m with and without 10 min irradiation at a fluence of 1.8 J/cm^2 . **A** 24 h incubation after photoirradiation; **B** 48 h incubation after photoirradiation. Non-photoirradiated CPT-DP plus DPc/m, filled square; photoirradiated CPT/m plus DPc/m, unfilled square. Data are shown as mean \pm SD ($n=4$).

properties (scattering light intensity, cumulant diameter and polydispersity index) of DPc/m were not changed during the photoirradiation under the tested conditions in this study (Supporting Information). The detailed intracellular behaviors of DPc/m are now under investigation, and the results will be reported elsewhere in the near future.

Recent developments in fiber optics and laser technology allow illuminating many sites inside the human body, e.g. gastrointestinal tract, urogenital organs, lungs, brain and pancreas. However, as for PDT, one important *in vivo* restriction is the limited penetration of light into the tissue. In tissues, the light penetration decays approximately exponentially (e^{-1}) for every 2–3 mm, with a theoretical maximum for PDT effects of about 1 cm if a photosensitizer that absorbs in the far-red region of the light spectrum is used (9). For PCI, the penetration depth would be substantially larger, since very good PCI effects can be achieved with very feeble light doses. Accordingly, the penetration depths of light for effective PCI could be expected at approximately 2 cm (9). In addition, in the PCI-mediated chemotherapy, chemotherapeutic agents released from the nanocarriers after photoirradiation can diffuse through the tumor tissue, allowing the treatment of thicker and hypoxic tumors, which are known to be intractable by PDT alone due to the limited light penetration and low oxygen concentration, respectively. Another benefit of PDT and chemotherapy combination is that PDT has shown to overcome multidrug resistance in many *in vivo* tumor models (43). Recent *in vitro* results indicated that PCI has the ability to circumvent the multidrug resistance in adriamycin-resistant breast cancer MCF-7 cells by release of the adriamycin localized at end-/lysosomes after PCI (42, 44, 45).

CONCLUSION

We have designed a novel PCI-activated drug carrier for the delivery of CPT using the glutathione-sensitive polymeric micelle. The micelle showed very low release of free drug under physiological conditions. However, in the presence of a reductive agent (DTT), the drug release increased rapidly. The effect of PCI strikingly enhances the *in vitro* cytotoxicity of CPT/m by augmenting the micelle access to the cytosol. The PCI employing the combinational micelle formulations of DPc/m and CPT/m could allow the long-sought ability to deliver chemotherapeutics where, when, and in the required doses, thus maximizing their effect and reducing side effects and damage to healthy tissues. The present results not only

Table I. *In Vitro* Cytotoxicity of Free Camptothecin, Thiolated Camptothecin, CPT-Loaded Micelles Plus 1×10^{-4} mg/ml of Dendrimer Phthalocyanine-loaded Micelles Against HeLa Cells

Irradiation (min)	Post-incubation (h)	IC50 (μM) ^a		
		CPT + DPc/m	CPT-DP + DPc/m	CPT/m + DPc/m
0	24	2	1	N.D.
0	48	1.5	0.4	65
10 ^b	24	1	0.7	20
10	48	1.5	0.2	10

CPT Camptothecin, CPT-DP thiolated camptothecin, CPT/m CPT-loaded micelles, DPc/m dendrimer phthalocyanine-loaded micelles

^a IC50 value obtained by 3-(4,5-dimethylthiazol-2-yl)-2,5-diphenyltetrazolium bromide assay

^b Cells were photoirradiated at a fluence of 1.8 J/cm^2

warrant the further development of CPT/m with respect to the optimization and the *in vivo* development, but also indicate the potential of the PCI technology applied to polymeric micelles that specifically release their contents under reductive conditions.

ACKNOWLEDGEMENT

This research was supported in part by the New Energy and Industrial Technology Development Organization of Japan (project code: P06042), Grant-in-Aid for Cancer Research from the Ministry of Education, Culture, Sports, Science and Technology as well as Grant-in-Aid for Cancer Research and Nanomedicine projects from Ministry of Health, labour and Welfare, Japan.

REFERENCES

1. N. K. Mal, M. Fujiwara, and Y. Tanaka. Photocontrolled reversible release of guest molecules from coumarin modified mesoporous silica. *Nature* **421**:350–353 (2003). doi:10.1038/nature01362.
2. A. Mueller, B. Bondurant, and D.F. O'Brien. Visible-light-stimulated destabilization of PEG-liposomes. *Macromolecules* **33**:4799–4804 (2000). doi:10.1021/ma0000551.
3. B. Bondurant, A. Mueller, and D. F. O'Brien. Photoinitiated destabilization of sterically stabilized liposomes. *Biochim. Biophys. Acta.* **1511**:113–122 (2001). doi:10.1016/S0005-2736(00)00388-6.
4. J. Lu, E. Choi, F. Tamanoi, and J. I. Zink. Light-activated nanoimpeller-controlled drug release in cancer cells. *Small* **4**:421–426 (2008). doi:10.1002/smll.200700903.
5. C. P. McCoy, C. Rooney, C. R. Edwards, D. S. Jones, and S. P. Gorman. Light-triggered molecule-scale drug dosing devices. *J. Am. Chem. Soc.* **129**:9572–9573 (2007). doi:10.1021/ja073053q.
6. K. Berg, P. K. Selbo, L. Prasmickaite, T. E. Tjelle, K. Sandvig, J. Moan, G. Gaudernack, Ø. Fodstad, S. Kjølrsrud, H. Anholt, G. H. Rodal, S. K. Rodal, and A. Høgset. Photochemical internalization: a novel technology for delivery of macromolecules into cytosol. *Cancer Res.* **59**:1180–1183 (1999).
7. P. K. Selbo, K. Sandvig, V. Kirveliēne, and K. Berg. Release of gelonin from endosomes and lysosomes to cytosol by photochemical internalization. *Biochim. Biophys. Acta.* **1475**:307–313 (2000).
8. A. Høgset, L. Prasmickaite, T. E. Tjelle, and K. Berg. Photochemical transfection: a new technology for light-induced, site-directed gene delivery. *Hum. Gene Ther.* **11**:869–880 (2000). doi:10.1089/10430340050015482.
9. A. Høgset, L. Prasmickaite, P. K. Selbo, M. Hellum, B. Ø. Engesæter, A. Bonsted, and K. Berg. Photochemical internalisation in drug and gene delivery. *Adv. Drug Deliv. Rev.* **56**:95–115 (2004). doi:10.1016/j.addr.2003.08.016.
10. N. Nishiyama, A. Iriyama, W-D. Jang, K. Miyata, K. Itaka, Y. Inoue, H. Takahashi, Y. Yanagi, Y. Tamaki, H. Koyama, and K. Kataoka. Light-induced gene transfer from packaged DNA enveloped in a dendrimeric photosensitizer. *Nat. Mater.* **4**:934–941 (2005). doi:10.1038/nmat1524.
11. N. Nishiyama, Arnida, W-D. Jang, K. Date, K. Miyata, and K. Kataoka. Photochemical enhancement of transgene expression by polymeric micelles incorporating plasmid DNA and dendrimer-based photosensitizer. *J. Drug Targeting* **14**:413–424 (2006). doi:10.1080/10611860600834508.
12. Arnida, N. Nishiyama, W-D. Jang, Y. Yamasaki, and K. Kataoka. Novel ternary polyplex of triblock copolymer, pDNA and anionic dendrimer phthalocyanine for photochemical enhancement of transgene expression. *J. Control. Release* **116**:e75–e77 (2006). doi:10.1016/j.jconrel.2006.09.058.
13. Arnida, N. Nishiyama, N. Kanayama, W-D. Jang, Y. Yamasaki, and K. Kataoka. PEGylated gene nanocarriers based on block cationomers bearing ethylenediamine repeating units directed to remarkable enhancement of photochemical transfection. *J. Control. Release* **115**:208–215 (2006).
14. K. R. Weishaupt, C. J. Gomer, and T. J. Dougherty. Identification of singlet oxygen as the cytotoxic agent in photoactivation of a murine tumor. *Cancer Res.* **36**:2326–2329 (1976).
15. H. I. Pass. Photodynamic therapy in oncology: mechanisms and clinical use. *J. Natl. Cancer Inst.* **85**:443–456 (1993). doi:10.1093/jnci/85.6.443.
16. S. B. Brown, E. A. Brown, and I. Walker. The present and future role of photodynamic therapy in cancer treatment. *Lancet Oncol.* **5**:497–508 (2004). doi:10.1016/S1470-2045(04)01529-3.
17. A. Meister, and M. E. Anderson. Glutathione. *Annu. Rev. Biochem.* **52**:711–760 (1983). doi:10.1146/annurev.bi.52.070183.003431.
18. K. Kataoka, A. Harada, and Y. Nagasaki. Block copolymer micelles for drug delivery: design, characterization and biological significance. *Adv. Drug Deliv. Rev.* **47**:113–131 (2001). doi:10.1016/S0169-409X(00)00124-1.
19. R. Duncan. The dawning era of polymer therapeutics. *Nature Rev. Drug Discov.* **2**:347–360 (2003). doi:10.1038/nrd1088.
20. N. Nishiyama, and K. Kataoka. Current state, achievements, and future prospects of polymeric micelles as nanocarriers for drug and gene delivery. *Pharmacol. & Ther.* **112**:630–648 (2006). doi:10.1016/j.pharmthera.2006.05.006.
21. A. Lavasanifar, J. Samuel, and G. S. Kwon. Poly(ethylene oxide)-block-poly(L-amino acid) micelles for drug delivery. *Adv. Drug Deliv. Rev.* **54**:169–190 (2002). doi:10.1016/S0169-409X(02)00015-7.
22. Y. Matsumura, and H. Maeda. A new concept for macromolecular therapeutics in cancer chemotherapy: mechanism of tumorotropic accumulation of proteins and the antitumor agent SMANCS. *Cancer Res.* **46**:6387–6392 (1986).
23. W-D. Jang, N. Nishiyama, G-D Zhang, A. Harada, D-L Jiang, S. Kawauchi, Y. Morimoto, M. Kikuchi, H. Koyama, T. Aida, and K. Kataoka. Supramolecular nanocarrier of anionic dendrimer porphyrins with cationic block copolymers modified with poly(ethylene glycol) to enhance intracellular photodynamic efficacy. *Angew. Chemie., Int. Ed.* **117**:423–427 (2005). doi:10.1002/ange.200461603.
24. W-D. Jang, Y. Nakagishi, N. Nishiyama, S. Kawauchi, Y. Morimoto, M. Kikuchi, and K. Kataoka. Polyion complex micelles for photodynamic therapy: Incorporation of dendritic photosensitizer excitable at long wavelength relevant to improved tissue-penetrating property. *J. Control. Release* **113**:73–79 (2006). doi:10.1016/j.jconrel.2006.03.009.
25. J. O'Leary, and F. M. Muggia. Camptothecins: a review of their development and schedules of administration. *Eur. J. Cancer* **34**:1500–1508 (1998). doi:10.1016/S0959-8049(98)00229-9.
26. B. C. Giovannella, N. Harris, J. Mendoza, Z. Cao, J. Liehr, and J. S. Stehlin. Dependence of anticancer activity of camptothecins on maintaining their lactone function. *Ann. New York Acad. Sci.* **922**:27–35 (2000).
27. N. Nishiyama, S. Okazaki, H. Cabral, M. Miyamoto, Y. Kato, Y. Sugiyama, K. Nishio, Y. Matsumura, and K. Kataoka. Novel cisplatin-incorporated polymeric micelles can eradicate solid tumors in mice. *Cancer Res.* **63**:8977–8983 (2003).
28. A. C. H. Ng, X. Li, and D. K. P. Ng. Synthesis and photophysical properties of nonaggregated phthalocyanines bearing dendritic substitutes. *Macromolecules* **32**:5292–5298 (1999). doi:10.1021/ma990367s.
29. A. Harada, and K. Kataoka. Formation of polyion complex micelles in an aqueous milieu form a pair of oppositely charged block copolymers with poly(ethylene glycol) segments. *Macromolecules* **28**:5294–5299 (1995). doi:10.1021/ma00119a019.
30. Y. Kakizawa, A. Harada, and K. Kataoka. Environment-sensitive stabilization of core-shell structured polyion complex micelle by reversible cross-linking of the core through disulfide bond. *J. Am. Chem. Soc.* **121**:11247–11248 (1999). doi:10.1021/ja993057y.
31. K. Miyata, Y. Kakizawa, N. Nishiyama, A. Harada, Y. Yamasaki, H. Koyama, and K. Kataoka. Block cationomer polyplexes with regulated densities of charge and disulfide cross-linking directed to enhance gene expression. *J. Am. Chem. Soc.* **126**:2355–2361 (2004). doi:10.1021/ja0379666.
32. K. Miyata, Y. Kakizawa, N. Nishiyama, Y. Yamasaki, T. Watanabe, M. Kohara, and K. Kataoka. Practically applicable cross-linked polyplex micelle with high tolerability against freeze-drying for *in vivo* gene delivery. *J. Control. Release.* **109**:15–23 (2005). doi:10.1016/j.jconrel.2005.09.043.

33. K. Berg, A. Dietze, O. Kaalhus, and A. Høgset. Site-specific drug delivery by photochemical internalization enhances the antitumor effect of Bleomycin. *Clin. Cancer Res.* **11**:8476–8485 (2005). doi:10.1158/1078-0432.CCR-05-1245.
34. R. Greenwald, A. Pendri, C. Conover, C. Gilbert, R. Yang, and J. Xia. Drug delivery systems. 2. Camptothecin-20-O- poly (ethylene glycol) ester transport forms. *J. Med. Chem.* **39**:1938–1940 (1996). doi:10.1021/jm9600555.
35. B. B. Lundberg. Biologically active camptothecin derivatives for incorporation into liposome bilayers and lipid emulsions. *Anti-cancer Drug Design.* **13**:453–461 (1998).
36. X. Liu, B. C. Lynn, J. Zhang, L. Song, D. Bom, W. Du, D.P. Curran, and T. G. Burke. A versatile prodrug approach for liposomal core-loading of water-insoluble camptothecin anticancer drugs. *J. Am. Chem. Soc.* **124**:7650–7661 (2002). doi:10.1021/ja0256212.
37. A. Shenderova, T. G. Burke, and S. P. Schwendeman. Stabilization of 10-hydroxycamptothecin in poly(lactide-co-glycolide) microsphere delivery vehicles. *Pharm. Res.* **14**:1406–1414 (1997). doi:10.1023/A:1012172722246.
38. B. Ertl, and P. Platzer. Poly(D,L-lactide-co-glycolide) microspheres for sustained delivery and stabilization of camptothecin. *J. Control. Release* **61**:305–317 (1999). doi:10.1016/S0168-3659(99)00122-4.
39. K. M. Tyner, S. R. Schiffman, and E. P. Giannelis. Nano-biohybrids as delivery vehicles for camptothecin. *J. Control. Rel.* **95**:501–514 (2004). doi:10.1016/j.jconrel.2003.12.027.
40. P. Opanasopit, M. Yokoyama, M. Watanabe, K. Kawano, Y. Maitani, and T. Okano. Block copolymer design for camptothecin incorporation into polymeric micelles for passive tumor targeting. *Pharm. Res.* **21**:2001–2008 (2004). doi:10.1023/B:PHAM.0000048190.53439.eb.
41. R. Barreiro-Iglesias, L. Bromberg, M. Temchenko, T. A. Hatton, A. Concheiro, and C. Alvarez-Lorenzo. Solubilization and stabilization of camptothecin in micellar solutions of pluronic-g-poly(acrylic acid) copolymers. *J. Control. Release.* **97**:537–549 (2004).
42. P.-J. Lou, P.-S. Lai, M.-J. Shieh, A. J. MacRobert, K. Berg, and S. G. Bown. Reversal of doxorubicin resistance in breast cancer cells by photochemical internalization. *Int. J. Cancer* **119**:2692–2698 (2006). doi:10.1002/ijc.22098.
43. P. S. Lai, P. J. Lou, C. L. Peng, C. L. Pai, W. N. Yen, M. Y. Huang, T. H. Young, and M. J. Shieh. Doxorubicin delivery by polyamidoamine dendrimer conjugation and photochemical internalization for cancer therapy. *J. Control. Release* **122**:39–36 (2007). doi:10.1016/j.jconrel.2007.06.012.
44. M. A. M. Capella, and L. S. Capella. A light in multidrug resistance: photodynamic treatment of multidrug-resistant tumors. *J. Biomed. Sci.* **10**:361–366 (2003). doi:10.1007/BF02256427.
45. D. K. Adigbli, D. G. G. Wilson, N. Farooqui, E. Sousi, P. Risley, I. Taylor, A. J. MacRobert, and M. Loizidou. Photochemical internalisation of chemotherapy potentiates killing of multidrug-resistant breast and bladder cancer cells. *Br. J. Cancer* **97**:502–512 (2007). doi:10.1038/sj.bjc.6603895.

